ELSEVIER

Journal of Organometallic Chemistry 575 (1999) 57–62

Journal of Organometallic Chemistry

The '1,2 to 1,2' cage carbon isomerisation in bisphosphine carbanickelaboranes: synthesis and spectroscopic and crystallographic characterisation of 1,2-Ph_2-4,4-$(PMe_2Ph)_2$-4,1,2-*closo*-$NiC_2B_9H_9$, 1,2-Ph_2-4,4-$(PEt_3)_2$-4,1,2-*closo*-$NiC_2B_9H_9$ and 1,2-Ph_2-4-(dppe)-4,1,2-*closo*-$NiC_2B_9H_9$ ☆

Rhona M. Garrioch, Petric Kuballa, Kristen S. Low, Georgina M. Rosair, Alan J. Welch *

Department of Chemistry, Heriot-Watt University, Edinburgh EH14 4AS, UK

Received 21 July 1998

Abstract

Reaction between Tl_2[7,8-Ph_2-7,8-*nido*-$C_2B_9H_9$] and $NiCl_2(PR_3)_2$ in CH_2Cl_2 affords three new carbanickelaboranes; **1,** R_3 = Me_2Ph; **2**, R = Et; **3**, $(PR_3)_2$ = dppe. The molecular structures of all these compounds were established as 1,2-Ph_2-4,4-$(PR_3)_2$-4,1,2-*closo*-$NiC_2B_9H_9$ by spectroscopic and crystallographic techniques. It is presumed that the first (transient) products of the reactions are the compounds 1,2-Ph_2-3,3-$(PR_3)_2$-3,1,2-*closo*-$NiC_2B_9H_9$ which rearrange to the observed species by a '1,2 to 1,2' C_{cage} atom isomerisation to relieve intramolecular overcrowding.

Keywords: Carbanickelaboranes; Skeletal rearrangements; Metalloboranes

1. Introduction

The isomerisation of carbaboranes and heterocarbaboranes has been known for more than 30 years. In carbaborane chemistry the classic isomerisation is the 1,2 → 1,7 isomerisation of $C_2B_{10}H_{12}$ at ca. 450°C [1] and the 1,7 → 1,12 isomerisation at ca. 700°C [2] (Scheme 1). Although there has been considerable speculation about the possible mechanisms of these rearrangements over many years [3], only recently has useful experimental evidence begun to be obtained. Thus, we have been fortunate in isolating an intermediate in the net 1,2 → 1,7 C_{cage} atom isomerisation of one icosahedral carbamolybdaborane to another (Scheme 2) [4], and we have begun to build up a detailed picture of the full 1,2 → 1,7 isomerisation process by following the movement of vertices with appropriate substituents [5]. This approach is of value because the particular systems with which we work are initially overcrowded and isomerise at much reduced temperatures relative to non-sterically hindered carbametallaboranes, thus ensuring the integrity of the vertex—substituent atom bond.

Whilst the 3,1,2-MC_2B_9 → 1,2,8-MC_2B_9 isomerisation of icosahedral carbametallaboranes (net 1,2 → 1,7 C_{cage} atom isomerisation) is most common, it is not the only isomerisation known. Specifically, a 3,1,2-MC_2B_9 → 4,1,2-MC_2B_9 rearrangement (termed the '1,2 → 1,2' isomerisation, Scheme 3) occurs when 3,3′-M-(1,2-Me_2-1,2-*closo*-$C_2B_9H_9)_2$ (M = Ni or Pd) is heated; when [3,3′-Ni-(1,2-Me_2-1,2-*closo*-$C_2B_9H_9)_2$]$^-$ is oxidised [6]; as one product when 3-Cp-3,1,2-*closo*-$CoC_2B_9H_{11}$ or its bis-C_{methyl} analogue is heated, and as the only product on

☆ Steric effects in heteroboranes. Part 22. For part 21 see F. Teixidor, C. Viñas, M.A. Flores, G.M. Rosair, A.J. Welch, A.S. Weller, Inorg. Chem. 37 (1998) 5394.

* Corresponding author. Tel.: +44-131-451-3217; fax: +44-131-451-3180; e-mail: a.j.welch@hw.ac.uk.

0022-328X/99/$ - see front matter
PII: S0022-328X(98)00957-7

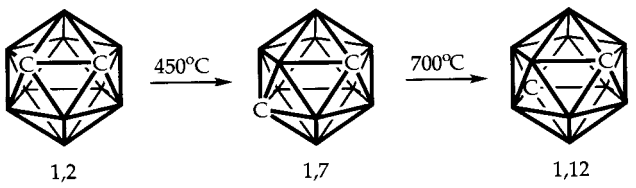

Scheme 1.

thermolysis of the C_{cage}-tied compound 1,2-$(CH_2)_3$-3-Cp-3,1,2-*closo*-$CoC_2B_9H_9$ [7]. Moreover, this rearrangement accompanies the decomposition of 1,2-Me_2-3,3-$(CO)_2$-3,1,2-*closo*-$NiC_2B_9H_9$ [8] and occurs at room temperature (r.t.) or below in certain bis(ligand) carbapalladaboranes [9]. In the 1,2→1,2 process one cage carbon atom moves away from the metal vertex but the C_{cage}–C_{cage} connectivity is retained. When thermally induced, such an isomerisation clearly follows a different pathway to the more common 1,2→1,7 C_{cage} atom isomerisation, but it should be possible to obtain useful experimental information on this pathway by using the same approach we are developing for the net 1,2→1,7 process, viz. low-temperature rearrangements induced by steric crowding and the use vertex-labelled carbaborane ligands.

We first require to identify a system that will undergo 1,2→1,2 isomerisation at low temperatures and in the absence of other reagents. Bis(phosphine) carbaplatinaboranes derived from $[7,8\text{-}Ph_2\text{-}7,8\text{-}nido\text{-}C_2B_9H_9]^{2-}$ show exclusively a net 1,2→1,7 C_{cage} atom isomerisation [10]. In this paper we demonstrate, through the synthesis and spectroscopic and structural study of three examples of 1,2-Ph_2-4,4-$(PR_3)_2$-4,1,2-*closo*-$NiC_2B_9H_9$, that analogous carbanickelaboranes undergo the desired 1,2→1,2 isomerisation.

2. Results and discussion

The straightforward reaction [11] between Tl_2[7,8-Ph_2-7,8-*nido*-$C_2B_9H_9$] and $NiCl_2(PR_3)_2$ in CH_2Cl_2 leads to the formation of the bisphosphine carbanickelaboranes 1,2-Ph_2-4,4-$(PR_3)_2$-4,1,2-*closo*-$NiC_2B_9H_9$ [**1**, R_3 = Me_2Ph; **2**, R = Et; **3**, $(PR_3)_2$ = dppe] in reasonable or good yields after chromatographic work up.

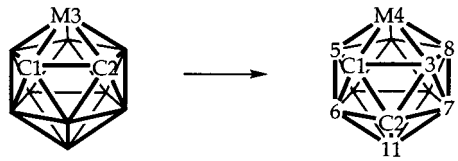

Scheme 3.

Compounds **1**–**3** are either green or red–brown solutions (dependent on solvent) and dark red solids. That they all have asymmetric structures is evident from ^{11}B- and ^{31}P-NMR spectroscopy. Thus, in the ^{11}B-{^{1}H} spectrum there are seven signals (5 × integral-1 and 2 × integral-2 coincidences) between +15 and −20 ppm, the range usually associated with *closo*-MC_2B_9 polyhedra. The ^{31}P-{^{1}H} spectra all reveal two resonances, resolved doublets in the case of **1** (J_{PP} 42 Hz) and **2** (J_{PP} 38 Hz), but broad unresolved single resonances in the case of compound **3**.

The molecular structures of compound **1**–**3** were established unambiguously by single crystal X-ray diffraction studies. In each case there is a single molecule in the asymmetric fraction of the unit cell. Perspective views of these molecules are given in Figs. 1–3, respectively, and Tables 1–3 report pertinent molecular parameters. All three structures are very similar. However, the precision of the structural study of **3** is significantly greater than that of **1** and **2**, as evidenced by e.g. estimated S.D.s on Ni–B distances (0.006 for **1**, 0.011 for **2** and 0.002 Å for **3**), reflecting the quality of the crystalline sample and the fact that diffraction data were collected at low temperature. For brevity, therefore, only the structure of **3** will be discussed in detail.

These structural studies confirm that the overall architecture of the new carbanickelaboranes is 4,1,2-*closo*-NiC_2B_9. Presumably metallation of the 7,8-*nido*-C_2B_9 ligand affords initially 3,1,2-*closo*-NiC_2B_9 species which are unacceptably sterically crowded and undergoes a spontaneous 1,2→1,2 isomerisation (Scheme 3). In compounds **1**–**3** the Ni(4) atom is located essentially centrally over the bonding B_4C face. That Ni–C(1) is the longest Ni–(face atom) distance reflects only the fact that the B_4C face is folded (by 7.7° in the case of compound **3**) into an envelope conformation with C(1) below the B(5,9,8,3) plane, and not a

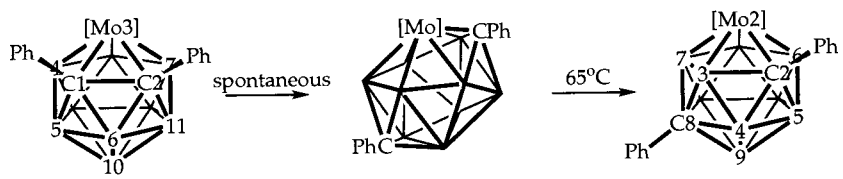

[Mo] = [Mo(η-C_3H_5)$(CO)_2$]$^-$

Scheme 2.

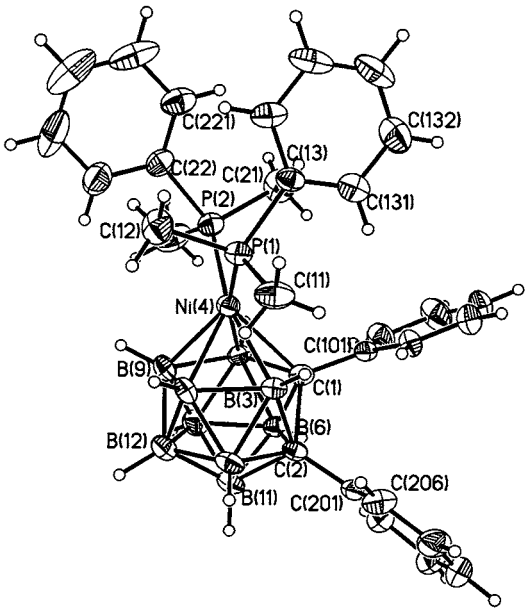

Fig. 1. Perspective view of a single molecule of compound **1**. Thermal ellipsoids are drawn at 30% probability level, except for H atoms. Phenyl rings numbered cyclically.

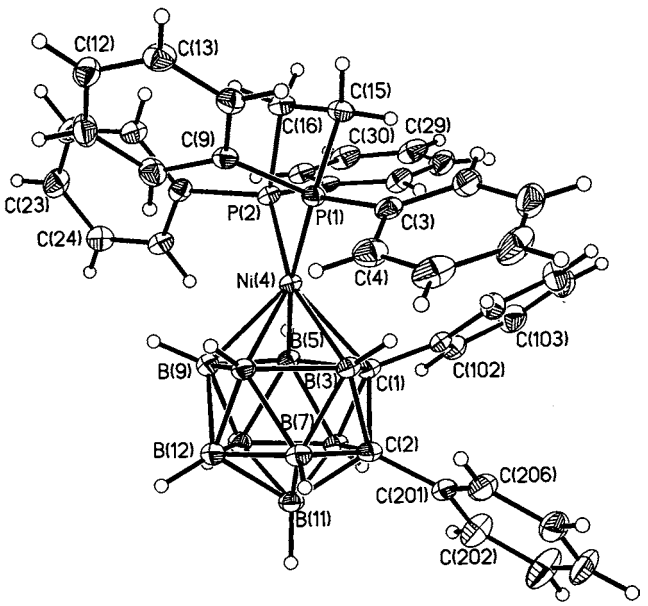

Fig. 3. Perspective view of a single molecule of compound **3**, drawn as for Fig. 1.

significant slippage [12] of the metal atom ($\Delta = 0.0$ Å) away from the C_{cage} atoms. The NiP_2 plane stands perpendicular to the vertical plane which bisects the B_4C face (dihedral angle 88.7° in **3**) and the conformation of the two C_{cage}-bound phenyl rings are described by very low θ values (11.6 and 7.9° for the rings of C(101) and C(201), respectively in **3**) measured relative to each other (θ is the modulus of the average C_{cage}–C_{cage}–C_{phenyl}–C_{phenyl} torsion angles [13]). Thus the $\{Ph_2C_2B_9\}$ portion of the molecule closely resembles

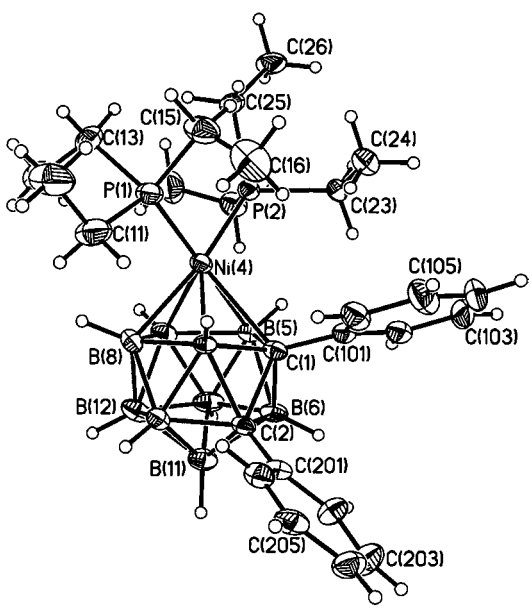

Fig. 2. Perspective view of a single molecule of compound **2**, drawn as for Fig. 1.

that in the parent species 1,2-Ph_2-1,2-*closo*-$C_2B_{10}H_{10}$ [14]. In compound **3** C(1)–C(2) is 1.693(2) Å.

The 4,1,2-*closo*-NiC_2B_9 architectures of compounds **1**–**3** show that bis(phosphine) 3,1,2-*closo*-NiC_2B_9 species with phenyl substituents on both cage carbon atoms {presumably the transient first products of the reactions between Tl_2[7,8-Ph_2-7,8-*nido*-$C_2B_9H_9$] and $NiCl_2(PR_3)_2$} undergo a net 1,2 → 1,2 C_{cage} atom isomerisation at r.t. or below. This is in marked contrast to the behaviour of analogous platinum species, where a net 1,2 → 1,7 C_{cage} atom isomerisation is observed [10], but presumably what drives both types of isomerisation is the relief of steric crowding in the 3,1,2-*closo*-MC_2B_9 precursor. To some degree, the involvement of steric crowding is also consistent with the known behaviour of bis(ligand)carbapalladaboranes. Stone et al. [9] have found that compounds 1,2-Me_2-3,3-L_2-3,1,2-*closo*-$PdC_2B_9H_9$ undergo a low-temperature (1,2 → 1,2) isomerisation for L_2 = (cod) and $(CO)_2$ but not for L_2 = tmeda, $(CN^tBu)_2$ and $(PMe_2Ph)_2$. This behaviour correlates ca. with the size of the slipping distortion Δ induced by the differing exo-polyhedral ligands. From model studies on 3,3-L_2-3,1,2-*closo*-$PdC_2B_9H_{11}$, Δ increases in the order L_2 = cod [15], $(PMe_3)_2$ [16], tmeda [16], as the π-acceptor strength of L decreases. One might reasonably expect that, everything else being equal, compounds with large Δ values would be less crowded than those with small Δ values, and thus less susceptible to isomerisation, which is what is observed.

Returning to the bis(phosphine) carbanickelaboranes **1**–**3**, the studies described herein demonstrate reliable, low-temperature 1,2 → 1,2 C_{cage} atom isomerisation. Future contributions [17] will report the synthesis and

structural characterisation of analogous compounds in which boron vertices are tagged with non-H substituents, which should help illuminate the isomerisation mechanism.

3. Experimental

3.1. Synthetic and spectroscopic

All experiments were performed under dry, oxygen-free N_2 using standard Schlenk techniques, with some subsequent manipulation in the open laboratory. Solvents were freshly-distilled over CaH_2 (CH_2Cl_2) or Na wire (40–60 petroleum ether, 60–80 petroleum ether). Preparative thin layer chromatography (TLC) employed 20 × 20 cm Kieselgel 60 F_{254} glass plates. NMR spectra at 400.1 (^{1}H), 162.0 (^{31}P) or 128.4 MHz (^{11}B) were recorded on a Bruker DPX 400 spectrometer, and ^{1}H spectra at 200.1 MHz on a Bruker AC 200 spectrometer, all as $CDCl_3$ solutions at ambient temperature. Elemental analyses were determined by the Departmental service (provided by Mr G. Evans). The starting materials Tl_2[7,8-Ph_2-7,8-*nido*-$C_2B_9H_9$] [18], $NiCl_2(PMe_2Ph)_2$, $NiCl_2(PEt_3)_2$ and $NiCl_2$(dppe) [19] were prepared by literature methods or slight variants thereof.

Table 1
Selected interatomic distances (Å) and interbond angles (°) for **1**

Interatomic distance (Å)			
Ni(4)–B(5)	2.080(6)	Ni(4)–B(3)	2.105(6)
Ni(4)–B(9)	2.111(6)	Ni(4)–B(8)	2.125(6)
Ni(4)–P(1)	2.202(2)	Ni(4)–P(2)	2.210(2)
Ni(4)–C(1)	2.304(5)	B(3)–C(1)	1.661(8)
B(3)–C(2)	1.784(8)	B(3)–B(7)	1.806(8)
B(3)–B(8)	1.829(9)	B(5)–C(1)	1.705(8)
B(5)–B(6)	1.788(8)	B(5)–B(10)	1.806(9)
B(5)–B(9)	1.855(9)	B(6)–C(2)	1.686(8)
B(6)–C(1)	1.706(8)	B(6)–B(11)	1.766(9)
B(6)–B(10)	1.787(9)	B(7)–C(2)	1.718(8)
B(7)–B(8)	1.772(9)	B(7)–B(12)	1.784(10)
B(7)–B(11)	1.794(9)	B(8)–B(9)	1.773(10)
B(8)–B(12)	1.787(9)	B(9)–B(12)	1.763(9)
B(9)–B(10)	1.775(10)	B(10)–B(11)	1.766(9)
B(10)–B(12)	1.769(11)	B(11)–C(2)	1.706(8)
B(11)–B(12)	1.748(9)	C(1)–C(101)	1.511(7)
C(1)–C(2)	1.681(7)	C(2)–C(201)	1.511(7)
Interbond angles (°)			
P(1)–Ni(4)–P(2)	97.01(6)	P(1)–Ni(4)–C(1)	122.78(14)
P(2)–Ni(4)–C(1)	116.8(2)	C(101)–C(1)–B(3)	121.72(16)
C(101)–C(1)–C(2)	117.07(15)	B(3)–C(1)–C(2)	62.80(12)
C(101)–C(1)–B(6)	115.28(16)	C(2)–C(1)–B(6)	60.02(12)
C(101)–C(1)–B(5)	123.35(16)	B(6)–C(1)–B(5)	63.24(12)
C(101)–C(1)–Ni(4)	116.16(13)	B(3)–C(1)–Ni(4)	63.00(9)
B(5)–C(1)–Ni(4)	62.11(9)	C(201)–C(2)–C(1)	118.56(16)
C(201)–C(2)–B(6)	121.13(17)	C(1)–C(2)–B(6)	60.49(12)
C(201)–C(2)–B(11)	121.58(16)	B(6)–C(2)–B(11)	62.59(13)
C(201)–C(2)–B(7)	119.51(16)	B(11)–C(2)–B(7)	63.17(13)
C(201)–C(2)–B(3)	117.99(16)	C(1)–C(2)–B(3)	58.53(11)
B(7)–C(2)–B(3)	61.91(12)		

Table 2
Selected interatomic distances (Å) and interbond angles (°) for **2**

Interatomic distances (Å)			
Ni(4)–B(3)	2.108(11)	Ni(4)–B(5)	2.111(12)
Ni(4)–B(8)	2.119(11)	Ni(4)–B(9)	2.163(11)
Ni(4)–P(1)	2.238(3)	Ni(4)–P(2)	2.246(3)
Ni(4)–C(1)	2.361(10)	C(1)–C(101)	1.503(14)
C(1)–B(3)	1.666(14)	C(1)–C(2)	1.683(12)
C(1)–B(6)	1.698(13)	C(1)–B(5)	1.73(2)
C(2)–C(201)	1.461(14)	C(2)–B(11)	1.70(2)
C(2)–B(7)	1.70(2)	C(2)–B(6)	1.70(2)
C(2)–B(3)	1.834(13)	B(3)–B(7)	1.802(14)
B(3)–B(8)	1.83(2)	B(5)–B(10)	1.81(2)
B(5)–B(6)	1.80(2)	B(5)–B(9)	1.83(2)
B(6)–B(10)	1.76(2)	B(6)–B(11)	1.76(2)
B(7)–B(8)	1.77(2)	B(7)–B(11)	1.78(2)
B(7)–B(12)	1.79(2)	B(8)–B(9)	1.77(2)
B(8)–B(12)	1.80(2)	B(9)–B(10)	1.77(2)
B(9)–B(12)	1.80(2)	B(10)–B(12)	1.77(2)
B(10)–B(11)	1.79(2)	B(11)–B(12)	1.75(2)
Interbond angle (°)			
P(1)–Ni(4)–P(2)	99.05(11)	P(1)–Ni(4)–C(1)	127.0(3)
P(2)–Ni(4)–C(1)	110.6(2)	C(101)–C(1)–B(3)	122.5(8)
C(101)–C(1)–C(2)	116.2(8)	B(3)–C(1)–C(2)	66.4(6)
C(101)–C(1)–B(6)	115.0(8)	C(2)–C(1)–B(6)	60.5(6)
C(101)–C(1)–B(5)	123.6(8)	B(6)–C(1)–B(5)	63.4(6)
C(101)–C(1)–Ni(4)	117.5(6)	B(3)–C(1)–Ni(4)	60.2(5)
B(5)–C(1)–Ni(4)	59.8(5)	C(201)–C(2)–C(1)	120.7(8)
C(201)–C(2)–B(7)	119.9(9)	B(11)–C(2)–B(7)	63.0(7)
C(1)–C(2)–B(6)	60.2(6)	B(11)–C(2)–B(6)	62.5(7)
C(201)–C(2)–B(3)	121.1(8)	C(1)–C(2)–B(3)	56.4(5)
B(7)–C(2)–B(3)	61.1(6)		

3.2. Synthesis of *1*

To a frozen (− 196°C) suspension of Tl_2[7,8-Ph_2-7,8-*nido*-$C_2B_9H_9$] (0.75 g, 1.08 mmol) in CH_2Cl_2 (20 cm^3), in a foil covered Schlenk tube, was added a solution of $NiCl_2(PMe_2Ph)_2$ (0.42 g, 1.08 mmol) in CH_2Cl_2 (20 cm^3), and the components re-frozen. The reaction mixture was then allowed to warm slowly to r.t. and stirred under N_2 overnight. The solid formed was removed by Schlenk filtration through Celite® from the deep red solution, from which the solvent was removed in vacuo to yield a thick, deep red oil. Initial purification by column chromatography (SiO_2, CH_2Cl_2) was followed by further purification by preparative TLC (1:1 CH_2Cl_2/40–60 petroleum ether). The mobile green band was collected.

Compound **1**, 1,2-Ph_2-4,4-$(PMe_2Ph)_2$-4,1,2-*closo*-$NiC_2B_9H_9$, yield = 0.48 g (71%). $C_{30}H_{41}B_9NiP_2$ requires C 58.2, H 6.67%. Found C 57.2, H 6.21%. ^{11}B-{^{1}H}-NMR, δ 11.08 (1B), 2.19 (1B), − 0.93 (1B), − 4.03 (1B), − 9.88 (2B), − 14.05 (2B) and − 15.39 (1B) ppm; ^{1}H-NMR, δ 7.45–6.25 (m, 20H, C_6H_5), 1.42 (d, 3H, CH_3, J_{PH} 8.9 Hz), 1.34 (d, 3H, CH_3, J_{PH} 8.6 Hz), 1.14

(d, 3H, CH_3, J_{PH} 8.6 Hz) and 1.13 (d, 3H, CH_3, J_{PH} 8.7 Hz) ppm; ^{31}P-{^1H}, δ −0.96 (d, J_{PP} 42 Hz) and −2.11 (d, J_{PP} 42 Hz) ppm. Dark red block crystals of diffraction quality were grown from diffusion of a CH_2Cl_2 solution of **1** and 40–60 petroleum ether (1:5).

3.3. Synthesis of **2**

Similarly, a suspension of Tl_2[7,8-Ph_2-7,8-*nido*-$C_2B_9H_9$] (0.75 g, 1.08 mmol) in CH_2Cl_2 (20 cm^3) was frozen to −196°C. To it was added a solution of $NiCl_2(PEt_3)_2$ (0.39 g, 1.08 mmol) in CH_2Cl_2 (20 cm^3) and the components were re-frozen. The reaction mixture was then allowed to warm slowly to r.t. and stirred overnight under N_2. Following filtration through Celite® a deep red filtrate was obtained, from which solvent was removed in vacuo to yield a thick, deep red oil. This was purified by preparative TLC (1:1 CH_2Cl_2/40–60 petroleum ether) which produced a single green band.

Compound **2**, 1,2-Ph_2-4,4-$(PEt_3)_2$-4,1,2-*closo*-$NiC_2B_9H_9$, yield was 0.45 g (72%). Microanalysis unreliable because of slow loss solvent of crystallisation. ^{11}B-{^1H}-NMR, δ 11.48 (2B), 2.95 (1B), −1.51 (1B), −5.39 (1B), −10.22 (2B), −14.68 (1B) and −16.12 (1B) ppm; ^1H-NMR: δ 7.45–6.90 (m, 10H, C_6H_5), 1.80 (m, CH_2, 6H), 1.65 (m, CH_2, 3H), 1.55 (m, CH_2, 3H), 1.10 (m, CH_3, 9H) and 0.75 (m, CH_3, 9H) ppm; ^{31}P-{^1H}-NMR, δ 11.43 (d, J_{PP} 38 Hz) and 8.51 (d, J_{PP} 38 Hz) ppm. Diffraction quality red block-like crystals were grown from diffusion of a CH_2Cl_2 solution and 40–60 petroleum ether.

Table 3
Selected interatomic distances (Å) and interbond angles (°) for **3**

Interatomic distance (Å)			
Ni(4)–B(5)	2.065(2)	Ni(4)–B(3)	2.077(2)
Ni(4)–B(8)	2.119(2)	Ni(4)–B(9)	2.142(2)
Ni(4)–P(1)	2.1706(6)	Ni(4)–P(2)	2.1803(6)
Ni(4)–C(1)	2.1978(19)	P(1)–C(3)	1.812(2)
P(1)–C(9)	1.825(2)	P(1)–C(15)	1.839(2)
P(2)–C(20)	1.833(2)	P(2)–C(26)	1.842(2)
P(2)–C(16)	1.853(2)	C(1)–C(101)	1.507(3)
C(1)–B(3)	1.689(3)	C(1)–C(2)	1.692(3)
C(1)–B(6)	1.709(3)	C(1)–B(5)	1.728(3)
C(2)–C(201)	1.506(3)	C(2)–B(6)	1.701(3)
C(2)–B(11)	1.709(3)	C(2)–B(7)	1.719(3)
C(2)–B(3)	1.762(3)	B(3)–B(7)	1.790(3)
B(3)–B(8)	1.844(3)	B(5)–B(10)	1.796(3)
B(5)–B(6)	1.802(3)	B(5)–B(9)	1.843(3)
B(6)–B(11)	1.772(3)	B(6)–B(10)	1.779(3)
B(7)–B(12)	1.781(3)	B(7)–B(8)	1.782(3)
B(7)–B(11)	1.796(3)	B(8)–B(9)	1.769(3)
B(8)–B(12)	1.797(3)	B(9)–B(10)	1.783(3)
B(9)–B(12)	1.786(3)	B(10)–B(12)	1.781(3)
B(10)–B(11)	1.789(3)	B(11)–B(12)	1.761(3)
Interbond angle (°)			
P(1)–Ni(4)–P(2)	87.39(2)	P(1)–Ni(4)–C(1)	124.11(5)
P(2)–Ni(4)–C(1)	118.83(5)	C(101)–C(1)–B(3)	121.72(16)
C(101)–C(1)–C(2)	117.07(15)	B(3)–C(1)–C(2)	62.80(12)
C(101)–C(1)–B(6)	115.28(16)	C(2)–C(1)–B(6)	60.02(12)
C(101)–C(1)–B(5)	123.35(16)	B(6)–C(1)–B(5)	63.24(12)
C(101)–C(1)–Ni(4)	116.16(13)	B(3)–C(1)–Ni(4)	63.00(9)
B(5)–C(1)–Ni(4)	62.11(9)	C(201)–C(2)–C(1)	118.56(16)

3.4. Synthesis of **3**

Similarly, to a frozen suspension of Tl_2[7,8-Ph_2-7,8-*nido*-$C_2B_9H_9$] (0.51 g, 0.73 mmol) in CH_2Cl_2 (20 cm^3) was added a solution of $NiCl_2$(dppe) (0.39 g, 0.73 mmol) in CH_2Cl_2 (20 cm^3). The mixture was then allowed to warm to r.t. and stirred overnight. The suspension was filtered through Celite® and the brown filtrate concentrated to ca. 5 cm^3 in vacuo. Preparative TLC on silica with CH_2Cl_2/60–80 petroleum ether (60:40) as eluent yielded a major product, **3**, as a red–brown band (R_f 0.48) and a minor product **4** as a red band (R_f 0.55).

Compound **3**, 1,2-Ph_2-4,4-(dppe)-4,1,2-*closo*-$NiC_2B_9H_9$, yield was 0.14 g (25%). $C_{40}H_{43}B_9NiP_2$ requires C 64.8, H 5.84%. Found C 63.2, H 5.81%. ^{11}B-{^1H}-NMR, δ 13.80 (2B), 1.64 (1B), −1.42 (1B), −4.04 (1B), −9.74 (2B), −12.21 (1B) and −14.83 (1B) ppm; ^1H-NMR, δ 7.83 (m, C_6H_5), 7.72 (m, C_6H_5), 7.56–6.60 (m, C_6H_5) and 2.22 (d, br, 4H, $Ph_2PCH_2CH_2PPh_2$) ppm; ^{31}P-{^1H}-NMR, δ 59.7 (br, s) and 55.7 (br, s) ppm. Red crystals of diffraction quality were obtained by slow diffusion of a CH_2Cl_2 solution and 40–60 petroleum ether at r.t.

3.5. Crystallographic

Single crystals of **1** and **2** were mounted in a subsequently sealed thin-walled glass capillary using epoxy resin glue and data were collected at r.t. (293 K). A crystal of **3** was coated in nujol and vacuum grease and mounted on a glass fibre; data were collected at 160 K using an Oxford Cryosystems Cryostream. All measurements were made on a Siemens P4 diffractometer using the program XSCANS [20], with data collection by ω scans. Standard reflections were re-measured every 100 data, but no significant crystal decay was found. Data were corrected for absorption by psi scans. All three structures were solved by direct and difference Fourier methods, and refined by full-matrix least squares against F^2. Non-hydrogen atoms were refined with anisotropic displacement parameters. Cage, phenyl and methyl H atom positions were calculated and treated as riding models with H atom displacement parameters $U_{iso\text{-}H}$ 1.2, 1.2 and 1.5 times the bound carbon or boron atom U_{eq}, respectively. The CH_2Cl_2 solvent molecule in the lattice of **2** was found to be partially disordered. Crystallographic computing was performed using the SHELXTL [21] system version 5.03 on a Pentium 90 MHz PC. Further details are given in Table 4.

Table 4
Crystallographic data for compounds **1**–**3**[a]

	1	**2**	**3**
Crystal habit	Plate	Block	Plate
Crystal size (mm)	$0.16\times0.36\times0.52$	$0.41\times0.23\times0.21$	$0.10\times0.42\times0.38$
Formula	$C_{30}H_{41}B_9NiP_2$	$C_{27}H_{51}B_9Cl_2NiP_2$	$C_{40}H_{43}B_9NiP_2$
M	619.57	664.52	741.68
System	Monoclinic	Monoclinic	Triclinic
Space group	$P2_1/c$	$P2_1/n$	$P\bar{1}$
a (Å)	12.2982(14)	10.306(2)	10.4690(10)
b (Å)	14.0427(11)	20.588(3)	11.3550(10)
c (Å)	19.484(3)	16.775(2)	16.739(2)
α (°)	90.00	90.00	93.620(10)
β (°)	104.380(12)	93.940(13)	101.250(10)
γ (°)	90.00	90.00	106.220(10)
U (Å^3)	3259.5(6)	3551.2(10)	1859.3(3)
Z	4	4	2
$D_{calc.}$	1.263	1.243	1.325
μ(Mo–K$_\alpha$) (mm^{-1})	0.714	0.805	0.639
$\theta_{data\ collection}$ (°)	1.71–25.00	1.57–25.00	2.08–25.00
Data measured	7061	7727	7713
Unique data	5657	6191	6545
Observed data [$I>2\sigma(I)$]	3038	3645	5901
R, wR_2 (observed data)	0.0602;0.1000	0.1015;0.2449	0.0336;0.0907
Variables	379	370	469
E_{max}, E_{min} (e Å^{-3})	0.308, −0.333	1.111, −0.438	0.357, −0.303

[a] $R=\Sigma\|\|F_o|-|F_c\|/\Sigma|F_o|$, $wR_2=[\Sigma[w(F_o^2-F_c^2)^2]/\Sigma w(F_o^2)^2]^{1/2}$, (where $w^{-1}=[\sigma_c^2(F_o)^2+(aP)^2+bP]$ and $P=[0.333\ \max\ \{F_o,\ 0\}+0.667\ (F_o)^2]$), $S=[\Sigma[w(F_o^2-F_c^2)^2/(n-p)]^{1/2}$, (where n is the number of data and p the number of parameters).

Acknowledgements

P. Kuballa is an ERASMUS-SOCRATES exchange student from the University of Münster, Germany. We thank the EPSRC for support (RMG) and the Callery Chemical Company for a generous gift of $B_{10}H_{14}$.

References

[1] D. Grafstein, J. Dvorak, Inorg. Chem. 2 (1963) 1128.
[2] S. Papetti, T.L. Heying, J. Am. Chem. Soc. 86 (1964) 2295.
[3] (a) W.N. Lipscomb, Science 153 (1966) 373. (b) L.I. Zakharkin, V.N. Kalinin, Dokl. Akad. Nauk SSSR 169 (1966) 590. (c) S. Wu, M. Jones, J. Am. Chem. Soc. 111 (1989) 5373. (d) G.M. Edvenson, D.F. Gaines, Inorg. Chem. 29 (1990) 1210. (e) Y.V. Roberts, B.F.G. Johnson, J. Chem. Soc. Dalton Trans. (1994) 759.
[4] S. Dunn, G.M. Rosair, Rh. LI. Thomas, A.S. Weller, A.J. Welch, Angew. Chem. Int. Ed. Engl. 36 (1997) 645.
[5] S. Dunn, G.M. Rosair, A.S. Weller, A.J. Welch, J. Chem. Soc. Chem. Commun. (1998) 1065.
[6] L.F. Warren, M.F. Hawthorne, J. Am. Chem. Soc. 92 (1970) 1157.
[7] M.K. Kaloustian, R.J. Wiersma, M.F. Hawthorne, J. Am. Chem. Soc. 93 (1971) 4912.
[8] N. Carr, D.F. Mullica, E.L. Sappenfield, F.G.A. Stone, Inorg. Chem. 33 (1994) 1666.
[9] K.A. Fallis, D.F. Mullica, E.L. Sappenfield, F.G.A. Stone, Inorg. Chem. 33 (1994) 4927.
[10] (a) D.R. Baghurst, R.C.B. Copley, H. Fleischer, D.M.P. Mingos, G.O. Kyd, L.J. Yellowlees, A.J. Welch, T.R. Spalding, D. O'Connell, J. Organomet. Chem. 447 (1993) C14. (b) G.O. Kyd, PhD Thesis (1993) University of Edinburgh.
[11] R.E. King, S.B. Miller, C.B. Knobler, M.F. Hawthorne, Inorg. Chem. 22 (1983) 3548.
[12] D.M.P. Mingos, M.I. Forsyth, A.J. Welch, J. Chem. Soc. Dalton Trans. (1978) 1363.
[13] J. Cowie, B.D. Reid, J.M.S. Watmough, A.J. Welch, J. Organomet. Chem. 481 (1994) 283.
[14] Z.G. Lewis, A.J. Welch, Acta Crystallogr. C49 (1993) 705.
[15] D.E. Smith, A.J. Welch, Acta Crystallogr. C42 (1986) 1717.
[16] H.M. Colquhoun, T.J. Greenhough, M.G.H. Wallbridge, J. Chem. Soc. Dalton Trans. (1985) 761.
[17] R.M. Garrioch, G.M. Rosair, A.J. Welch (1998) in preparation.
[18] Z.G. Lewis, A.J. Welch, J. Organomet. Chem. 430 (1992) 45.
[19] G. Booth, J. Chatt, J. Chem. Soc. (1965) 3238.
[20] Siemens Analytical Instruments, Inc. (1994) Madison, Wisconsin, USA.
[21] G.M. Sheldrick, SHELXTL/PC. Siemens Analytical X-ray Instruments Inc. (1994) Madison, Wisconsin, USA.